Al_3O_n and $Al_3O_n^-$ ($n = 1-3$) Clusters: Structures, Photoelectron Spectra, Harmonic Vibrational Frequencies, and Atomic Charges

Ana Martínez,* Luis E. Sansores, Roberto Salcedo, and Francisco J. Tenorio

Instituto de Investigaciones en Materiales, UNAM, Circuito Exterior s/n, C. U., P.O. Box 70-360, Coyoacán, 04510, D.F. México

J. V. Ortiz

Department of Chemistry, Kansas State University, Manhattan, Kansas 66506-3701

Received: May 30, 2002; In Final Form: August 28, 2002

Structure and bonding in Al_3O_n and $Al_3O_n^-$ aluminum oxide clusters where $n = 1-3$ are studied with electronic structure calculations and are compared with some experimental results. Geometry optimizations with the B3LYP/6-311+G(2d,p) density functional method produced minima which were verified with frequency calculations. Several initial geometries and distinct spin multiplicities were considered for each case. The most stable anionic structures from density functional calculations were confirmed with additional geometry optimizations at the QCISD level. Equilibrium geometries, harmonic frequencies, and atomic charges are presented. These results, in combination with previous assignments of anion photoelectron spectra, provide a consistent explanation for changes in isomerization energies between anionic and neutral species.

Introduction

Aluminum oxides occur in many ceramics and catalytic supports. Bonding interactions in these compounds between oxygen and aluminum are chiefly ionic.[1] For solid Al_2O_3, valence electrons of Al are transferred to O atoms, thus producing closed-shell Al^{3+} and O^{2-} ions whose electrostatic interactions are the principal component of the resulting insulator's cohesive energy. These ionic interactions are expected in Al_xO_y clusters as well. For a given x, the transformation from metallic to ionic bonding may be observed with increasing y. Aluminum-rich species, where x/y exceeds 2/3, are especially pertinent to interfaces between bulk Al_2O_3 and metallic phases. Moreover, combustion and oxidation of aluminum lead to the presence of many intermediates whose structure and reactivity motivate intense study.

Hypermetallic molecules with metal oxidation numbers that are less than normal may consist of metal clusters bound ionically to a nonmetallic central atom. Aluminum−oxygen clusters in this class have been studied experimentally and theoretically.[2−4] For example, AlO, the simplest aluminum oxide cluster, has been studied in the gas phase by various methods.[5−8] Electron propagator calculations and configuration interaction calculations have succeeded in obtaining accurate electron detachment energies of AlO^-.[9] Thermochemical relationships involving several aluminum−oxygen clusters have been examined computationally.[10] Theoretical studies of Al_3O have been reported as an example of hypermetalated species.[3,4] There have been many experimental studies of small aluminum oxide cluster,[11,12] including a systematic photoelectron spectroscopy study of $Al_3O_y^-$, where $y = 0-5$.[13] In the latter work, Wu et al. reported that the electron affinity of neutral Al_3O_y clusters increases with O content. Low-energy features in the photoelectron spectra corresponding to Al-centered orbitals become less numerous with increasing y, thus demonstrating the evolution of electronic structure from the metallic limit, Al_3, to the oxide limit, Al_3O_5. Anion photoelectron spectra suggest that two electrons from Al_3 clusters are transferred to each O atom to make O^{2-}. These transfers produce a very high electron affinity for Al_3O_5, which requires one electron to complete the set of 10 required for five O atoms. For several of these anions, the presence of more than one isomer has been inferred from the variation of relative peak intensities with respect to laser fluence and ion-source conditions. A photoisomerization between two isomers of $Al_3O_3^-$ was observed under high detachment laser fluences.

Photoelectron spectroscopy is an informative probe of molecular electronic structure. Accurate treatments of electron correlation often are needed to produce a quantitative interpretation of the most intense spectral features. Determination of the order of final states and concomitant assignments may require correlated levels of theory. Some final states may not correspond even qualitatively to the predictions of uncorrelated theories. Recently, Ganthy and Davidson[14] performed calculations on Al_3O and its anion; these results have been used to interpret the photoelectron spectrum of Al_3O^-. To explain the features of the photoelectron spectra of $Al_3O_2^-$ and $Al_3O_3^-$, they reported[15] ground-state geometries of neutral and anionic forms of Al_3O_2 and Al_3O_3 and energies of the low-lying states of Al_3O_2 and Al_3O_3.

Electron propagator theory provides a framework for the systematic inclusion of electron correlation in a one-electron picture of molecular electronic structure. Propagator calculations produce Dyson orbitals and correlated electron binding energies without determining wave functions and energies of individual states. Several approximate propagators have been derived and have been shown to be accurate and efficient tools for the computation of vertical and adiabatic electron binding energies. The association of Dyson orbitals to electron binding energies

* Corresponding author.

10.1021/jp0213102 CCC: $22.00
Published on Web 10/05/2002

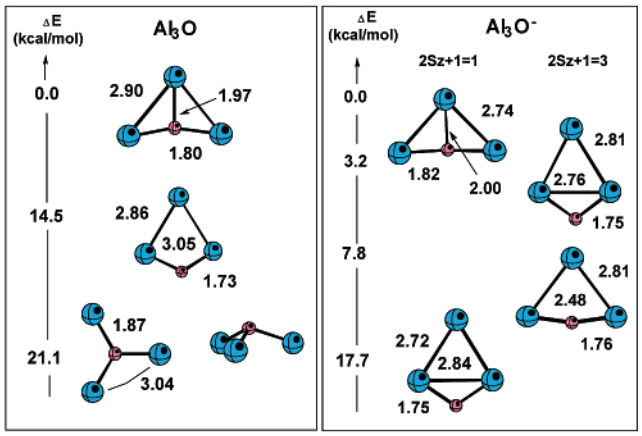

Figure 1. Optimized Al_3O and Al_3O^- structures. Bond distances in Å. Energy differences in kcal/mol.

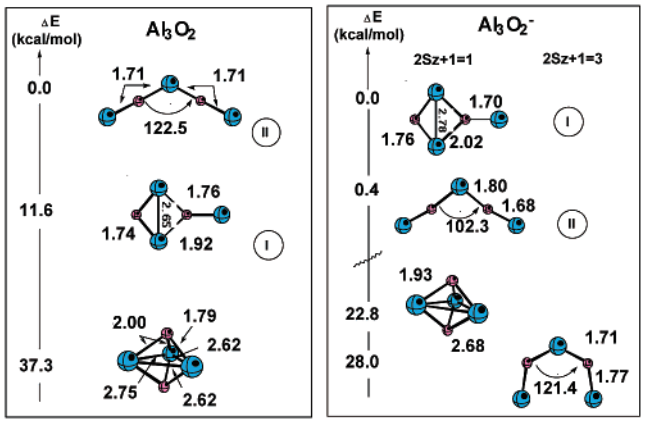

Figure 2. Optimized Al_3O_2 and $Al_3O_2^-$ structures. Bond distances in Å. Energy differences in kcal/mol.

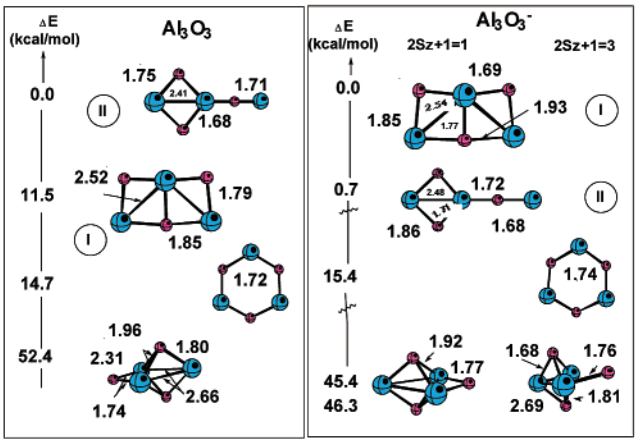

Figure 3. Optimized Al_3O_3 and $Al_3O_3^-$ structures. Bond distances in Å. Energy differences in kcal/mol.

facilitates interpretation of electronic structure in terms of one-electron concepts.[16] In previous works,[17,18] we reported ground-state geometries and energies of the low-lying states of neutral and anionic forms of Al_3O, Al_3O_2, and Al_3O_3. Electron propagator calculations on cluster electron binding energies were used to assign the photoelectron spectra. With these results, an improved understanding of these experiments was obtained. The structure and bonding of the clusters were discussed on the basis of spectral data and calculated geometries and energies.

In this paper, we attempt to discuss stable structures of Al_3O_n and $Al_3O_n^-$, ($n = 1-3$). Optimized geometries, harmonic vibrational frequencies, and isomerization energies are presented. Using the ionization energies obtained in a previous work with electron propagator calculations, the relative energies of Al_3O_n and $Al_3O_n^-$ isomers are explained.

Computational Details

All calculations have been carried out using the program Gaussian 98.[19] Full geometry optimization without symmetry constraints was performed using density functional (DF) calculations. Hybrid B3LYP[20] density functional calculations were performed with the 6-311+G(2d,p) basis.[21] Optimized geometries were verified with frequency calculations. To locate distinct minima on potential energy surfaces, full geometry optimization has been performed, starting from several initial geometries. Different spin multiplicities ($2S_z + 1$) were considered as well. One cannot exclude the possibility that true global minima were missed in the optimization procedure, but the diversity of initial geometries and spin multiplicities that were considered is sufficient to inspire confidence that the global minimum has been identified.

The most stable anionic structures from DF calculations were reexamined with additional geometry optimizations at the QCISD[22] level; 6-311G(d) and 6-311+G(2d) basis sets were used.[21] QCISD geometries were assumed in subsequent electron propagator calculations of the vertical electron detachment energies (VEDEs) of the anions with 6-311+G(2df) and 6-311+G(3d2f) basis sets.[21] See references 17 and 18 for details.

Geometry Optimization

Many initial geometries with different bond distances and angles were tested for each structure. For each anion and neutral radical, several stationary points on each potential energy surface were found. Figures 1−3 present the most stable neutral and anionic structures for Al_3O, Al_3O_2, and Al_3O_3, respectively.

For Al_3O, there are two stable structures, with an energy difference of 14.5 kcal/mol. For the anionic system, the structures present different spin multiplicities (singlet and triplet). The ground state is a singlet. The singlet−triplet splitting is 3.2 kcal/mol, and there is also another triplet at 7.8 kcal/mol. In a previous work,[17] we reported the re-optimized structures at the QCISD/6-311G(2df) level. Discrepancies between DF and QCISD bond lengths are 0.02 Å or less; QCISD values are slightly smaller. Whereas the singlet structure of the anion is lower than the triplet form by 3.2 kcal/mol in DF optimizations, the QCISD energy difference is 4.5 kcal/mol. Similar results were reported by Boldyrev and Schleyer,[3] whose optimized neutral Al_3O structures at the HF/6-31G* and MP2/6-31G* levels are quite similar to the most stable structure of Figure 1.

For Al_3O_2, two different C_{2v} minima are shown in Figure 2. The energy difference between the neutral structures is 11.6 kcal/mol. For the ground state, there are no Al−Al bonds of the kind that occur in the aluminum trimer or in Al_3O. For the anionic system, there are two structures with similar stability. Both are singlets and the energy difference between them is 0.4 kcal/mol. Because this value is very small, we cannot say with certainty that one isomer is more stable than the other. The planar triplet is 28.0 kcal/mol higher in energy. For Al_3O_2 and $Al_3O_2^-$, there are stable D_{3h} forms, which lie at 37.3 and 22.8 kcal/mol, respectively, above the minimum. Planar geometries are preferred over three-dimensional ones. Ghanty and Davidson, in another DF[15] study of Al_3O_2 and $Al_3O_2^-$, found similar structures. For the neutral, their energy difference between the two lowest doublets was 12.2 kcal/mol. For the

TABLE 1: Al_3O^-. VEDEs (eV)

initial state (energy)[a]	final state	BD-T1[c] (p)[b]	ΔQCISD(T)[e]	PES[d]
$1A_1$	$^2B_2$	1.20		1.22 X′
(0.0)		(0.87)		
	$^2A_1$	3.39		3.5 B
		(0.82)		
	$^2B_2$	3.86		4.2 C
		(0.80)		
	$^2A_1$	5.03		5.0 D
		(0.42)		
$^3B_1$	$^2A_1$		1.55	1.68 X
(0.19)	$^2B_1$		1.67	1.68 X
	$^4B_1$		2.94	3.0 A
$^2A_2$	$^2B_2$		1.00	1.22 X′
(0.39)	$^2B_1$		1.57	1.68 X
	$^4A_2$		3.27	3.5 B

[a] QCISD/6-311G(d) relative energies of anions. [b] Pole strengths. [c] BD-T1/6-311+G(3d2f) VEDEs. [d] Anion photoelectron spectra.[13] [e] QCISD(T)/6-311+G(2df) VEDEs.

anion, their energy difference between the two lowest singlets was 0.39 kcal/mol. These values are in good agreement with the present results. For $Al_3O_2^-$, the two lowest C_{2v} singlets were re-optimized at the QCISD/6−311(d) level. As we reported before,[17] the QCISD energy difference is 3.6 kcal/mol (0.16 eV) and it exceeds the DF value by 3.2 kcal/mol. Discrepancies between DF and QCISD bond lengths are 0.02 Å or less.

For Al_3O_3, two different C_{2v} minima are presented in Figure 3. The energy difference between the neutral structures is 11.5 kcal/mol. For the anionic system, there are two isomers with similar stability. Both are singlets and the energy difference between them is 0.7 kcal/mol. This value is very small and we cannot certify that one structure is more stable than the other. The planar triplet is 15.4 kcal/mol higher in energy. For Al_3O_3 and $Al_3O_3^-$, there are stable three-dimensional minima at 52.4 and 45.4 kcal/mol above their respective minimum-energy geometries. Planar structures are preferred over three-dimensional ones. Ghanty and Davidson, in their DF[15] study of Al_3O_3 and $Al_3O_3^-$, found similar geometries. For the neutral, their energy difference between the two lowest doublets is 11.1 kcal/mol; for the anion, their energy difference between the two lowest singlets is 0.87 kcal/mol. These values are also in good agreement with the present results. The two lowest singlets of $Al_3O_3^-$ were re-optimized at the QCISD/6-311G(d) level. The energy difference between the singlets is 4.6 eV instead of 0.7 kcal/mol with DF energies. DF and QCISD bond lengths agree within 0.01 Å of each other, as we reported in a previous paper.[17]

Photoelectron Spectra

Experimental data by Wu et al.[13] and some previously reported theoretical results[17] on the VEDEs of Al_3O^-, $Al_3O_2^-$, and $Al_3O_3^-$ are presented in Tables 1−3, respectively. Electron propagator and QCISD(T) results for the VEDEs of the singlet and the lowest triplet of Al_3O^- are in close agreement with anion photoelectron spectra. This assignment was achieved without the employment of empirical factors and provided an explanation for the relative intensities of the most prominent peaks. A similar computational strategy leads to structures I and II of Figure 2 for $Al_3O_2^-$ which are very close in energy. For Al_3O_2, there are two similar structures, but structure II is clearly lower in energy. Combination of electron propagator results for the two isomers provides an excellent account of the anion photoelectron spectrum. For $Al_3O_3^-$, there are two structures with nearly identical energies. The union of electron propagator VEDE predictions for the two isomers also gives a satisfactory description of the $Al_3O_3^-$ photoelectron spectrum.

TABLE 2: $Al_3O_2^-$. VEDEs (eV)

geometry (energy)[a]	final state	BD-T1[c] (p)[b]	PES[d]
structure I	$^2B_2$	2.38	2.29 X
(0.0)		(0.89)	
	$^2A_1$	3.55	3.5 A
		(0.88)	
	$^2A_1$	5.31	5.1 C
		(0.88)	
	$^2B_1$	6.04	
		(0.85)	
structure II	$^2A_1$	2.06	1.8 X′
(0.16)	$^2B_2$	(0.88)	
		4.83	4.7 B
	$^2A_1$	(0.89)	
		5.15	
	$^2B_2$	(0.88)	
		6.36	
		(0.85)	

[a] QCISD/6-311G(d) relative energies of anions. [b] Pole strengths. [c] BD-T1/6-311+G(2df) VEDEs. [d] Anion photoelectron spectra.[13]

TABLE 3: $Al_3O_3^-$. VEDEs (eV)

geometry (energy)[a]	final state	BD-T1[c] (p)[b]	PES[d]
structure I	$^2B_2$	3.07	2.96 X
(0.0)		(0.89)	
	$^2A_1$	3.73	3.7 A
		(0.89)	
structure II	$^2A_1$	2.36	2.25 X′
(0.20)		(0.89)	
	$^2B_2$	5.37	5.2 B
		(0.87)	
	$^2A_2$	5.46	5.2 B
		(0.86)	
	$^2A_1$	6.15	
		(0.90)	

[a] QCISD/6-311G(d) relative energies of anions. [b] Pole strengths. [c] BD-T1/6-311+G(2df) VEDEs. [d] Anion photoelectron spectra.[13]

For Al_3O, the anion and the neutral systems present similar ground-state structures, but for Al_3O_2 and Al_3O_3, anion and neutral ground-state structures are different. Structure I is preferred by $Al_3O_2^-$. However, after removal of an electron, structure II is energetically lower. Structure I is preferred for $Al_3O_3^-$, but structure II is more stable for Al_3O_3.

Qualitative relationships between anion VEDEs and potential energy surfaces can now be explained. For Al_3O^-, Figure 4 shows schematic potential energy surfaces for the anionic and the neutral compounds. Experimental VEDEs and DF energy differences for the anions are shown. The triplet's structure possesses a larger VEDE than the singlet's. For this reason, the lowest structure of the neutral is similar to that of the anion. The neutral isomerization energy which is inferred from this scheme, 0.6 eV, is close to the calculated value shown in Figure 1, 14.5 kcal/mol.

For $Al_3O_2^-$, Figure 5 shows the potential energy surfaces for the anionic and the neutral compounds. Similar stabilities were found for I and II singlet anionic structures with DF calculations. However, the experimental VEDE for structure II is 1.8 eV, whereas for structure I this quantity is 2.3 eV. It is energetically easier to remove an electron from structure II than from structure I. The potential energy minimum of neutral II is lower than that of neutral minimum I. This argument explains the differences between II−I isomerization energies of Al_3O_2 and $Al_3O_2^-$.

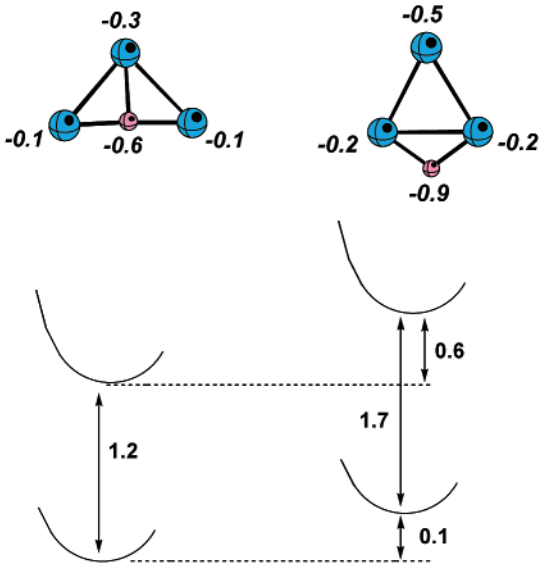

Figure 4. Schematic representation of the potential energy surfaces for the most stable structures of Al_3O (neutral and anionic). Values are energy differences in eV.

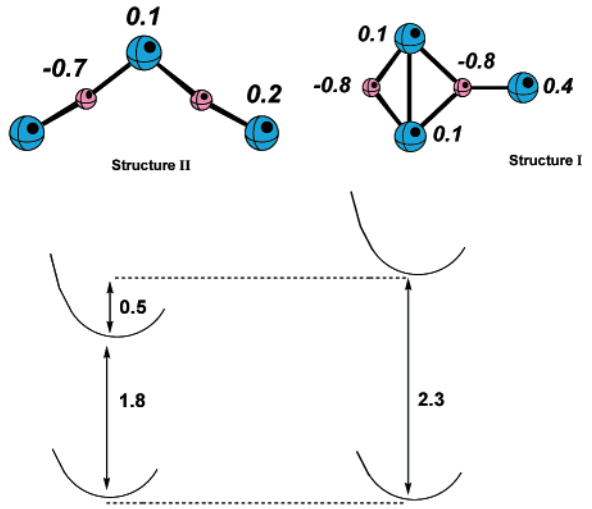

Figure 5. Schematic representation of the potential energy surfaces for the most stable structures of Al_3O_2 (neutral and anionic). Values are energy differences in eV.

The neutral isomerization energy is 0.5 eV, in close agreement with the estimate of Figure 2, 11.6 kcal/mol.

For $Al_3O_3^-$, the explanation is similar. In Figure 6, schematic potential energy surfaces for the most stable neutral and anionic structures are presented. The VEDE of anion II is lower than the VEDE of anion I. Therefore, structure II is more stable than structure I for the neutral system. The energy difference between the Al_3O_3 minima obtained with the VEDEs (0.8 eV) is somewhat larger than the energy difference between the optimized neutral structures (0.5 eV) shown in Figure 3. This discrepancy is chiefly due to neglect of differences in relaxation energies in the two, neutral potential energy surfaces.

Vibrational Analysis and Atomic Charges

DF optimizations and electron propagator calculations have produced accurate VEDEs in close agreement with photoelectron spectra. Reliable ground-state structures for these systems can be inferred from these results. For Al_3O, Al_3O_2, and Al_3O_3, Ghanty and Davidson found similar structures.[14,15] An additional triplet with C_{2v} symmetry also was found in our work on Al_3O^-.[17]

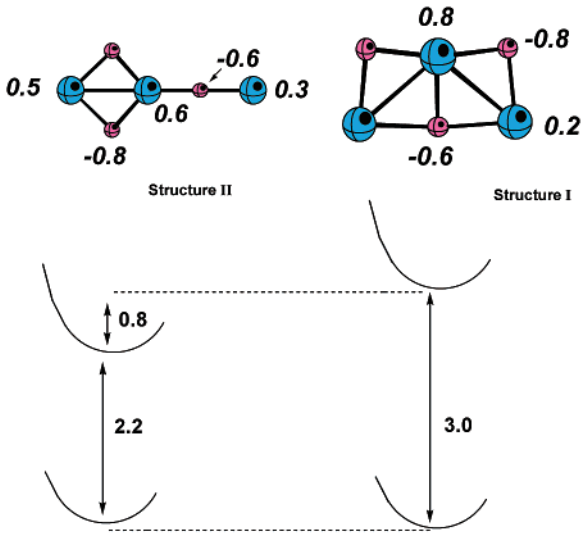

Figure 6. Schematic representation of the potential energy surfaces for the most stable structures of Al_3O_3 (neutral and anionic). Values are energy differences in eV.

TABLE 4: Calculated Harmonic Vibrational Frequencies (in cm^{-1}) of Low-Energy Isomers of Al_3O and Al_3O^-. Mulliken Atomic Charges Are Also Included

Al_3O ΔE=O	0.1, 0.3, -0.7, 0.3					
Frequency	147	150	155	347	407	625
symmetry	b_2	b_1	a_1	a_1	a_1	b_2
Al_3O^- ΔE=0.0	-0.3, -0.1, -0.6, -0.1					
Frequency	163	204	251	343	431	661
symmetry	b_1	a_1	b_2	a_1	a_1	b_2
Al_3O^- ΔE=3.2	-0.5, -0.2, -0.2, -0.9					
Frequency	120	166	215	259	662	679
symmetry	b_2	b_1	a_1	a_1	b_2	a_1

Harmonic vibrational frequencies and Mulliken atomic charges are shown in Tables 4−6 for the most stable neutral and anionic structures of Al_3O, Al_3O_2, and Al_3O_3, respectively. All structures are minima on their potential energy surfaces.

In Table 4, atomic charges of Al_3O and Al_3O^- indicate that the oxygen atom is negative, as expected from the electronegativities of oxygen and aluminum. For the anionic system, the

TABLE 5: Calculated Harmonic Vibrational Frequencies (in cm^{-1}) of Low-Energy Isomers of Al_3O_2 and $Al_3O_2^-$. Mulliken Atomic Charges Are Also Included

Al_3O_2 ΔE=0.0	 Structure II								
Frequency	38	76	84	96	238	452	569	992	1012
symmetry	a_1	b_2	a_2	b_1	a_1	a_1	b_2	a_1	b_2
Al_3O_2 ΔE=11.6	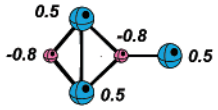 Structure I								
Frequency	97	106	154	227	334	419	667	720	793
symmetry	b_2	b_1	b_2	b_1	a_1	a_1	b_2	a_1	a_1
$Al_3O_2^-$ ΔE=0.0	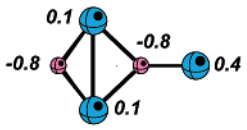 Structure I								
Frequency	65	86	179	203	271	359	678	743	845
symmetry	b_2	b_1	b_1	b_2	a_1	a_1	a_1	b_2	a_1
$Al_3O_2^-$ ΔE=0.4	 Structure II								
Frequency	34	70	81	86	233	438	458	962	983
symmetry	a_1	b_2	a_2	b_1	a_1	a_1	b_2	b_2	a_1

TABLE 6: Calculated Harmonic Vibrational Frequencies (in cm^{-1}) of Low-Energy Isomers of Al_3O_3 and $Al_3O_3^-$. Mulliken Atomic Charges Are Also Included

Al_3O_3 ΔE=0.0	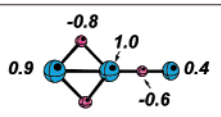 Structure II											
Frequency	39	57	172	234	344	362	591	642	751	769	804	1068
symmetry	b_2	b_1	b_1	b_2	a_1	b_1	a_1	b_2	a_1	b_2	a_1	a_1
Al_3O_3 ΔE=11.5	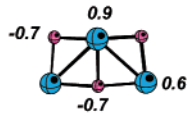 Structure I											
Frequency	100	181	247	301	337	434	560	575	583	645	729	980
symmetry	b_1	a_2	a_1	b_2	b_1	a_1	b_2	b_2	A_1	A_1	a_1	b_2
$Al_3O_3^-$ ΔE=0.0	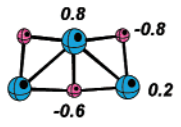 Structure I											
Frequency	109	171	206	336	357	416	462	538	575	691	742	997
symmetry	b_1	a_2	a_1	b_1	b_2	a_1	b_2	a_1	b_2	a_1	a_1	b_2
$Al_3O_3^-$ ΔE=0.7	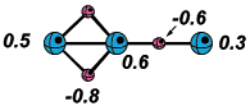 Structure II											
Frequency	23	45	147	227	326	335	494	546	601	823	846	1046
symmetry	b_2	b_1	b_1	b_2	a_1	b_1	b_2	a_1	a_1	b_2	a_1	a_1

aluminum atoms present a small negative charge, while in the neutral species the aluminum atoms have positive charges. The changes in atomic charges are compatible with the Al-centered Dyson orbital that corresponds to the lowest VEDE of the singlet anion.[17]

For Al_3O_2 and $Al_3O_2^-$, Table 5 shows that the charge on the aluminum atoms is positive for the neutral and for the anionic systems, but is it less positive for the anionic systems. If one compares the neutral and anionic I structures, the charges of the aluminums that are equivalent by symmetry in the anion are 0.1, whereas in the neutral system these charges are 0.5. The Coulombic repulsion between these two atoms is higher for the neutral than for the anionic structure. This effect contributes to the stability order of the two isomers. For the anionic system, structures I and II have similar stability. The Coulombic repulsion between the two equivalent Al atoms is small. For the neutral system, the Coulombic repulsion between the equivalent Al atoms is larger and this structure is less stable than the neutral ground state by 11.6 kcal/mol. The Dyson orbital for the lowest VEDE of the structure I anion comprises Al hybrid lobes with opposite phases and smaller, antibonding contributions from bridging O p orbitals. Removal of an electron from this orbital therefore produces smaller internuclear separations in the four-member ring. (See Figure 2.) The Coulombic destabilization of isomer I is a consequence of phase relationships in the Dyson orbital.

In Table 6, the results for Al_3O_3 and $Al_3O_3^-$ indicate that aluminum atoms are positive, but again the charge is less positive for the anionic systems. The Coulombic repulsion between the aluminum atoms is larger in the neutral structure I than in the anionic structure I. In these structures, the central Al repels the two symmetry-equivalent Al atoms and in the neutral, two such interactions are accentuated. The neutral structure I is less stable than structure II because the Coulombic repulsion between the aluminum atoms is larger. In the anionic system, there is less Coulombic repulsion and structure I is as stable as structure II. The Dyson orbital for the lowest VEDE of the anion structure I consists of lobes with opposite phases on the two, symmetry-equivalent Al atoms and smaller, antibonding contributions from O p orbitals. Electron density therefore is removed chiefly from the two equivalent Al atoms.

Conclusions

Density functional optimizations produce C_{2v} structures for doublet Al_3O and singlet Al_3O^-, respectively. The singlet−triplet splitting for the latter species is small. Similar patterns of stability occur for the neutral and anionic structures. For the Al_3O_2 anionic system, structures I and II are very close in energy. For neutral Al_3O_2, there are two similar structures, but structure II is clearly lower in energy. Al_3O_3 presents two isomers, I and II. For the anions, these structures are very close in energy. After removal of an electron, form II is energetically preferred. Subsequent QCISD optimizations confirm all the anion results. Electron propagator and QCISD(T) results for the VEDEs are in close agreement with anion photoelectron spectra.

A vibrational analysis and Mulliken atomic charges were reported for the more stable neutral and anionic structures of Al_3O, Al_3O_2, and Al_3O_3. All structures are minima on their respective potential energy surfaces. The stability order of the anionic and neutral compounds may be explained by Coulombic repulsions between aluminum atoms. For $Al_3O_2^-$ and $Al_3O_3^-$, the aluminum atoms are less positive and the Coulombic repulsion is lower than for the neutral, where the aluminum atoms are more positive and the Coulombic repulsion is large.

For these reasons, neutral and anionic systems exhibit different ground-state geometries.

Acknowledgment. The authors acknowledge Sara Jiménez Cortés and María Teresa Vázquez for technical support and DGSCA/UNAM (México) for providing computer time. This work was partially funded by DGAPA (# IN107399) and CONACYT-NSF (E120.1778/2001). J.V.O. acknowledges support from the National Science Foundation (Grants CHE-9873897 and CHE-0135823) and Kansas DEPSCoR.

References and Notes

(1) Henrich, V. E; Cox, P. A. *The Surface Science of Metal Oxides*. Cambridge University Press: New York, 1994.

(2) Cox, D. M.; Trevor, D. J.; Whitten, R. L.; Rohlfing, E. A.; Kaldor, A. J. *J. Chem. Phys.* **1986**, *84*, 4651.

(3) Boldyrev, A. I.; Schleyer, P. v. R. *J. Am. Chem. Soc.* **1991**, *113*, 9045.

(4) Zakrzewski, V. G.; Niessen, W. v.; Boldyrev, A. I.; Schleyer, P. v. R. *Chem. Phys. Lett.* **1993**, *174*, 167.

(5) Rosenwaks, S.; Steele, R. E.; Broida, H. P. *J. Chem. Phys.* **1975**, *63*, 1963.

(6) Hebert, T.; Schriever, U.; Kolb, D. M. *Chem. Phys. Lett.* **1992**, *200*, 258.

(7) Dagdigian, P. J.; Cruse, H. W.; Zare, R. N. *J. Chem. Phys.* **1975**, *62*, 1824.

(8) Sayers, M. J.; Gole, J. L. *J. Chem. Phys.* **1977**, *67*, 5442.

(9) (a) Ortiz, J. V. *Chem. Phys. Lett.* **1998**, *296*, 494. (b) Zenouda, C.; Blottiau, P.; Chambaud, G.; Rosmus, P. *J. Mol. Struct. (THEOCHEM)* **1999**, *458*, 61.

(10) Politzer, P.; Lane, P.; Grice, M. E. *J. Phys. Chem. A* **2001**, *105*, 7473.

(11) Desai, S. R.; Wu, H.; Wang, L. S. *Int. J. Mass Spectrom. Ion Process.* **1996**, *159*, 75.

(12) Desai, S. R.; Wu, H.; Rohfling, C.; Wang, L. S. *J. Chem. Phys.* **1997**, *106*, 1309.

(13) Wu, H.; Li, X.; Wang, X. B.; Ding, C. F.; Wang, L. S. *J. Chem. Phys.* **1998**, *109*, 449.

(14) Ghanty, T. K.; Davidson, E. R. *J. Phys. Chem.* **1999**, *103*, 2867.

(15) Ghanty, T. K.; Davidson, E. R. *J. Phys. Chem.* **1999**, *103*, 8985.

(16) (a) Ortiz, J. V. In *Computational Chemistry: Reviews of Current Trends*; Leszczynski, J., Ed.; World Scientific: Singapore, 1997; Vol. 2, p 1. (b) Ortiz, J. V. *Adv. Quantum Chem.* **1999**, *35*, 33. (c) Ortiz, J. V.; Zakrzewski, V. G.; Dolgounitcheva, O. In *Conceptual Trends in Quantum Chemistry*; Kryachko, E. S., Ed.; Kluwer: Dordrecht, 1997; Vol. 3, p 465.

(17) Martínez, A.; Tenorio, F. J.; Ortiz. J. V. *J. Phys. Chem. A* **2001**, *105*, 8787.

(18) Martínez, A.; Tenorio, F. J.; Ortiz, J. V. *J. Phys. Chem. A* **2001**, *105*, 11291.

(19) Frisch, M. J.; Trucks, G. W.; Schlegel, H. B.; Scuseria, G. E.; Robb, M. A.; Cheeseman, J. R.; Zakrzewski, V. G.; Montgomery, J. A., Jr.; Stratmann, R. E.; Burant, J. C.; Dapprich, S.; Millam, J. M.; Daniels, A. D.; Kudin, K. N.; Starin, M. C.; Farkas, O.; Tomasi, J.; Barone, V.; Cossi, M.; Cammi, R.; Mennucci, B.; Pomelli, C.; Adamo, C.; Clifford, S.; Ochterski, J.; Petersson, G. A.; Ayala, P. Y.; Cui, Q.; Morokuma, K.; Malick, D. K.; Rabuck, A. D.; Raghavachari, K.; Foresman, J. B.; Cioslowski, J.; Ortiz, J. V.; Stefanov, B. B.; Liu, G.; Liashenko, A.; Piskorz, P.; Komaromi, I.; Gomperts, R.; Martin, R. L.; Fox, D. J.; Keith, T.; Al-Laham, M. A.; Peng, C. Y.; Nanayakkara, A.; González, C.; Challacombe, M.; Gill, P. M. W.; Chen, W.; Wong, M. W.; Andres, J. L.; Head-Gordon, M.; Replogle, E. S.; Pople, J. A. *GAUSSIAN 98*, (Revision A8); Gaussian Inc.: Pittsburgh, PA, 1998.

(20) (a) Becke, A. D. *J. Chem. Phys.* **1993**, *98*, 5648. (b) Lee, C.; Yang, W.; Parr, R. G. *Phys. Rev. B* **1988**, *37*, 785. (c) Mielich, B.; Savin, A.; Stoll, H.; Preuss, H. *Chem. Phys. Lett.* **1989**, *157*, 200.

(21) (a) Krishnan, R.; Binkley, J. S.; Seeger, R.; Pople, J. A. *J. Chem. Phys.* **1980**, *72*, 650. (b) Clark, T.; Chandrasekhar, J.; Spitznagel, G. W.; Schleyer, P. v. R. *J. Comput. Chem.* **1983**, *4*, 294. (c) Frisch, M. J.; Pople, J. A.; Binkley, J. S. *J. Chem. Phys.* **1984**, *80*, 3265. (d) McLean, A. D.; Chandler, G. S. *J. Chem. Phys.* **1980**, *72*, 5639.

(22) Pople, J. A.; Head-Gordon, M.; Raghavachari, K. *J. Chem. Phys.* **1987**, *87*, 5968.